

Interatom intrashell blockade

L. Sælen, S. I. Simonsen, and J. P. Hansen

Department of Physics and Technology, University of Bergen, N-5007 Bergen, Norway

(Received 10 August 2010; published 7 January 2011)

We demonstrate a feature of the Rydberg blockade mechanism which occurs between two *initially excited* circular Rydberg atoms. When both atoms are exposed to weak time-dependent electric fields, it is shown that the intrashell dynamics of each atom is strongly modified by the presence of the other. Three characteristic dynamical regimes are identified with separating radii which both scale linearly with principal quantum number n for otherwise constant field parameters. A region of conditional entangled electron dynamics is separated from the outer asymptotic region of independent atom dynamics through a conditional radius, R_c . An inner region, where both atoms becomes locked in their initial state, is again separated from the conditional region by a smaller blocking radius, R_b .

DOI: 10.1103/PhysRevA.83.015401

PACS number(s): 32.80.Rm, 03.65.Ud, 03.67.—a

About 10 years ago it was discovered that the large dipole moment of Rydberg states of interacting atoms can induce a detuning which effectively prohibits more than a single atom to become optically excited within a given volume [1,2]. Thus, in an atomic cloud exposed to a driving optical excitation scheme, the dipole-dipole interaction sets up an entangled multiparticle state with special correlation properties. Recently, the dipole blockade mechanism has been measured in controlled two-atom experiments with high-lying Rydberg states of rubidium [3,4] as well as in cold gases [5–7]. In addition to the fascinating exploration of exotic quantum dynamics in mesoscopic systems, the dipole blockade opens for applications within quantum information [8]. Here a number of quantum gates based on single-atom gates and conditional two-atom gates and protocols involving a large number of atoms have been proposed [9].

Isolated Rydberg atoms can be experimentally prepared in almost any given linear combinations of spherical l, m states of a given principal quantum number n , including circular states (magnetic quantum number $m = \pm(n-1)$), coherent elliptical states (corresponding to classical states of fixed eccentricity [10]), or strongly polarized Stark states (Stark quantum number $k \sim n$) [11–13]. Experiments where recent progress has realized trapping and probing of conditional dynamics of two single atoms may therefore also probe intrashell dynamics of two initially excited Rydberg atoms. From the point of view of optical driving frequencies between ground-state atoms $|g\rangle$ and a single Rydberg level $|e\rangle$, the dynamics of this setup seems at first sight only to amount to a trivial phase development, as the combined initial state in fact is the dipole blocked dark state $|ee\rangle$ of the optical excitation scheme. However, when considering the response of Rydberg atoms to weak, time-dependent electric and magnetic fields, it is clear that for these interactions the initial state couple effectively to a manifold of intrashell states $|e_i, e_j\rangle$. In fact, the isolated atom intrashell dynamics can be completely controlled and driven between certain initial and final states with 100% transition probability for any n level [14].

In this Brief Report we explore the possibility of conditional dynamics between two Rydberg atoms based on numerical simulations and we show that the intrashell interatom dynamics can effectively generate entangled states due to a strong state sensitivity of the dipole-dipole interaction. Three

characteristic regimes are identified: An asymptotic region of isolated atom dynamics is separated from an intermediate region by a boundary R_c , where the two-atom dynamics is correlated, conditional and entangled. Inside the latter region there exists a third region, separated from the outside by R_b , where the dynamics of each atom becomes blocked by the strong dipolar interaction. The radial boundaries separating these regions will be shown to obey particular simple scaling relations with principal quantum number n .

Due to the SO(4) symmetry of the Coulomb problem the Hamiltonian of a single hydrogenic Rydberg atom with principal quantum number n can be expressed in terms of two general spins which interact with corresponding effective fields ω_{\pm} ,

$$h_0 = -\frac{1}{2n^2} + \tilde{\omega}_+ \tilde{J}_+ + \tilde{\omega}_- \tilde{J}_-. \quad (1)$$

Here $\omega_{\pm} = 1/2B(t) \pm 3/2nE(t)$, where $B < n^{-4}$, $E < 1/3n^{-5}$ describe weak time-dependent electric and magnetic fields in the limit where no mixing of adjacent n manifolds occurs [15]. The dimension of the two independent spins J_{\pm} is $(n-1)/2$ and can be expressed as a sum of $(n-1)$ spin $1/2$ systems according to the Majorana theorem [16]. Thus, the description of isolated atom intrashell dynamics in hydrogenic Rydberg atoms is reduced from an n^2 -basis state system to the evolution of two spin- $1/2$ systems precessing in two generalized fields ω_{\pm} .

The SO(4) symmetry becomes broken when two or more atoms interact. For two initially excited Rydberg atoms a product space of n, l_i, m_i, l_j, m_j states with i, j assigning all n^4 combinations of diatomic electronic states needs to be considered. This scaling fast creates a prohibitive computational problem even in the case of utilizing special molecular symmetries [17] and limits numerical simulations to rather small ($n < 20$ – 25) Rydberg states. However, in the setup to be discussed, the results scale with principal quantum numbers and can therefore be predicted for any pair of initial n levels. In the case of two atoms separated by a distance $\vec{R} = [0, 0, R]$, the Hamiltonian becomes

$$H = \sum_{i=1,2} h_0^i + V(r_a, r_b, R). \quad (2)$$

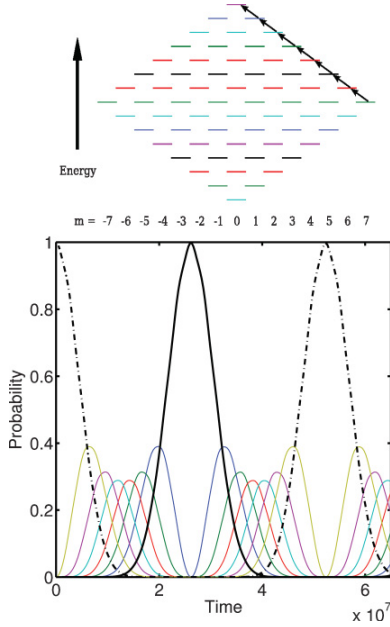


FIG. 1. (Color online) Illustration of microwave transitions from a circular to a polarized Stark state of the $n = 8$ Stark manifold (upper panel). The lower panel shows the time development in atomic units of the initial circular state (thick black dash-dotted line) and the maximal polarized Stark state (thick black line) as function of time for the electric field. The other populated six Stark states are shown in various thin color (gray scale) lines. Parameters: $|E_z| = 10^{-7}$, $\epsilon_0 = 0.1E_z$.

We approximate the diatomic interaction by the dipole-dipole interaction which is the leading asymptotic term

$$V(r_a, r_b, R) = \frac{x_a x_b + y_a y_b - 2z_a z_b}{R^3}, \quad (3)$$

where $r_{a,b}$ are the electron coordinates of each atom. Here and throughout atomic units are used.

In the crossed field setup [12,13] the Rydberg atoms are exposed to a constant electric field in the \hat{z} direction which generate Stark energy splitting $3/2nE_z$ as displayed in Fig. 1 for $n = 8$. A microwave field $E_{\perp}(t) = \epsilon_0[\cos(\omega t), \sin(\omega t), 0]$ drive transitions between the states according to the $|\Delta m| = 1$ selection rule, as illustrated in the upper panel of Fig. 1 with arrows starting from the circular $(k, m) = (0, 7)$ state. In general, when ω equals the Stark energy splitting, the transitions become resonant and n photon absorption from an initially circular state with Stark quantum numbers $(k, m) = (0, n - 1)$ will bring the system to the highest polarized Stark state $(k, m) = (n - 1, 0)$ in a time $T_{\text{rev}}/2 = 2\pi/3n\epsilon_0$. In twice the time the system periodically return to the initial state with unit probability. The population of the top Stark state appears as a resonance with an increasingly narrower width

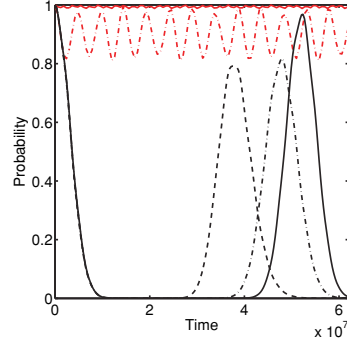


FIG. 2. (Color online) Time development in atomic units of the most circular ($m = 1$) initial state of two atoms in the $n = 8$ principal shell separated a distance R : Full red (gray) line, $R = 600$; dotted red (gray) line, $R = 800$; full black line, $R = 5000$; dash-dot black line, $R = 3000$; dashed black line, $R = 2000$. Electric field parameters as in Fig. 1.

for increasing n and can be traced back to the Majorana decomposition [14]. Between the resonances a large number of states are involved, as seen from Fig. 1.

Next we turn to the two-atom system and solve the time-dependent Schrödinger equation for the $n = 8$ case, keeping two atoms initially in the most circular state and a fixed interatomic distance R . The full black line in Fig. 2 shows the probability for the system to remain in the initial state for a near asymptotic interatomic distance $R \gg R_c$. A complete revival of the initial state is observed after $T \sim 5 \times 10^7$ a.u., as expected from the isolated atom case of Fig. 1. When reducing the interatom distance to $R = 3000$ and $R = 2000$ we observe still a full depletion of the initial state but only partial revivals. At even smaller interatomic distances, illustrated by red lines, the initial state remains more and more populated for all times, and a locking radius where the time dependence is almost entirely a phase development of the initial state can be defined.

We now consider the probability, P_{ee} , for both atoms to climb the Stark ladder from the initial circular state to the highest polarized Stark state for the same electric field parameters as in Fig. 2 and for the largest internuclear distances considered there (the black lines of Fig. 2). First, we observe for reference, a unit probability at $T_{\text{rev}}/2$ at the near asymptotic distance $R = 5000$. For the smaller distance, $R = 3000$, P_{ee} is less than 0.25 and at distances $R < 2000$, $P_{ee} \approx 0$. Then, in the middle panel of Fig. 3 we correspondingly plot the probability for excitation of a single atom only combination with one atom in the ground state or a lower excited state, P_e . In the asymptotic case this probability increases initially, as expected from Fig. 1, before it depletes as the top Stark state becomes resonant. For the smaller radii, $R = 2000, 3000$ the situation is strikingly different: Here, single-atom excitation remains dominant, $P_e \sim 0.5$, in the region where $P_{ee} \sim 0$. This illustrates that the dipole blockade mechanism plays a decisive role for intrashell dynamics of excited Rydberg atoms.

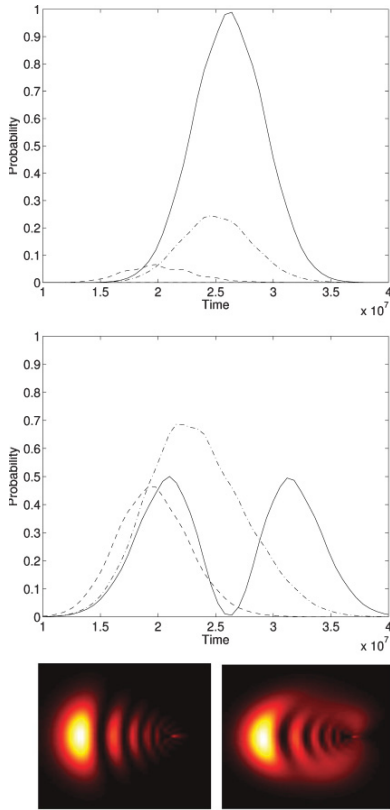


FIG. 3. (Color online) (Upper panel) Probabilities as function of time in atomic units for populating two atoms in the most polarized Stark state of the $n = 8$ manifold for three interatom distances $R = 5000$ (full lines), $R = 3000$ (dash-dotted line), and $R = 2000$ (dashed line, curve multiplied with a factor 1000). (Middle panel) Corresponding probability for single atom excitation. (Lower panel) Single electron density around each atom at $t = 2.5 \times 10^7$ for $R = 5000$ (left) and $t = 2.0 \times 10^7$ for $R = 2000$ (right). In the lower panel the horizontal z axis and the vertical y axis range from -150 to 50 a.u..

In the lower panel of Fig. 3 we display the scaled electronic density distribution $\rho(x_a, 0, z_a) = \int d^3r_b |r_a \Psi(x_a, 0, z_a, r_b)|^2$ of each atom at the half time before the first (partial) revival at $R = 5000$ (left) and $R = 2000$ (right), taken as snapshots of two movies of the time development [18]. In the asymptotic case the well-known image of a strongly polarized Stark state evolves and stabilizes around $t = T_{\text{rev}}/2$. In the interacting case the dominant population of entangled states induce a characteristic oscillation of the charge cloud in the region where it is stationary in the noninteracting case. In addition the electronic density becomes more diffuse.

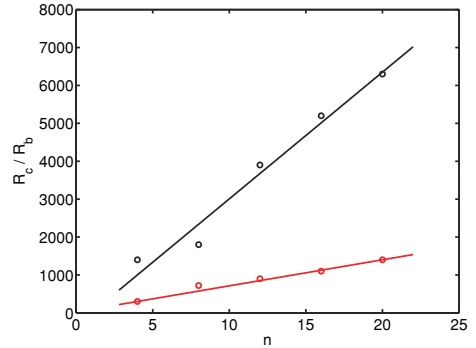


FIG. 4. (Color online) Conditional radius R_c in red (gray) and blocking radius R_b in black for fixed field parameters of Fig. 1. The circles are computational results for $n = 4, 8, 12, 16, 20$, while the solid lines are linear fits to the simulation data.

The results of Figs. 2 and 3 have displayed the following: Two $n = 8$ Rydberg atoms can be blocked and undergo conditional and unconditional dynamics for increasing interatomic distance. To generalize to an arbitrary pair of n levels we now loosely define the blocking radius R_b such that the initial state probability within this radius is never smaller than 0.9 and a conditional radius R_c such that the highest polarized Stark state probability $P_{ee}(t) < 0.1$ at any time. The scaling properties for fixed electric field parameters can then be investigated. Performing calculations up to $n = 20$ (160 000 states) and displaying the results in Fig. 4, we observe a near linear scaling of the two radii, which can be qualitatively understood from the following simple model: By assuming the dipole-dipole interaction to scale proportional to the product of characteristic Stark quantum number $k_{i,j}$ of each state, $\sim n^4 k_i k_j / R^3$, the two radii can be related to the energy splitting of the Stark ladder. This leads to a linear n dependence,

$$R_{c,b} \sim \left(\frac{2k_i k_j}{3E_z} \right)^{1/3} n, \quad (4)$$

a slope linear in n and characterized by the relevant Stark quantum numbers. It seems reasonable to take $k_i = k_j = 7$ in the case of $n = 8$ for R_c and $k_i = k_j = 1$ for R_b , which correspond respectively to blocking of a product of the most excited and the first excited levels on the Stark ladder of Fig. 1. This gives a ratio of between the slopes as $R_c/R_b = 3.7$, in fair agreement with the results of Fig. 4, $R_c/R_b \sim 4.5$. We also note from Eq. (4) that by taking E_z equal to a small fixed fraction of the energy splitting between two principal n levels, and thus remaining in the weak field limit for higher n levels, $E_z \sim n^{-3}$, we obtain a characteristic n^2 scaling of the two radii.

With the development of improved experimental setups to trap and store Rydberg atoms [19] the ability to conditionally access the intrashell dynamics of each atom imply that proposals for encoding quantum bits and phase operations

in principle can be adopted from well-known schemes of and ensemble of ground state and Rydberg atoms [9]. For example, the circular state can adopt the role of the ground state $|g\rangle \rightarrow |k,m\rangle = (0,l)$ and $|e\rangle \rightarrow |l,0\rangle$ defining an excited state of the qubit. Alternatively, new quantum “multibit schemes” [20] may be designed by taking advantage of the freedom to transfer the isolated Rydberg atom between at least four states with unit probability. Each Rydberg atom can then correspondingly store at least two qubits. One qubit could be coded in two opposite angular momenta defined by the (maximal) magnetic quantum number. The other can be coded in opposite polarizations given by the Stark quantum number, k . In this setup both qubits may be addressed independently by varying electric fields.

In conclusion, we have demonstrated from first-principle calculations that interatom intrashell dynamics opens a new

regime of dipole-dipole controlled electron dynamics between Rydberg atoms. Inside a characteristic radius, any Rydberg n level of two atoms develop conditional dynamics prohibiting the highest (lowest) energy Stark state of both atoms to be populated. Instead the atoms are entangled with a dominant state involving the most polarized Stark state of one of the atoms only. An additional characteristic feature of the system is a complete locking of the initial state for sufficient small interatomic distance. When controlled trapping of two Rydberg atoms can be achieved the remaining interaction parameters are in principle simple to realize. Entangled intrashell dynamics may then exhibit new possibilities for quantum information with neutral atoms.

This research has been supported by the Research Council of Norway (RCN).

-
- [1] D. J. D. Jaksch, J. I. Cirac, P. Zoller, S. L. Rolston, R. Côté, and M. D. Lukin, *Phys. Rev. Lett.* **85**, 2208 (2000).
- [2] M. D. Lukin, M. Fleischhauer, R. Côté, L. M. Duan, D. Jaksch, J. I. Cirac, and P. Zoller, *Phys. Rev. Lett.* **87**, 037901 (2001).
- [3] E. Urban, T. A. Johnson, T. Henage, L. Isenhower, D. D. Yavuz, T. G. Walker, and M. Saffman, *Nat. Phys.* **5**, 110 (2009).
- [4] A. Gaëtan, Y. Miroshnychenko, T. Wilk, A. Chotia, M. Viteau, D. Comparat, A. B. P. Pillet, and P. Grangier, *Nat. Phys.* **5**, 115 (2009).
- [5] D. Tong, S. M. Farooqi, J. Stanojevic, S. Krishnan, Y. P. Zhang, R. Côté, E. E. Eyler, and P. L. Gould, *Phys. Rev. Lett.* **93**, 063001 (2004).
- [6] K. Singer, M. Reetz-Lamour, T. Amthor, L. G. Marcassa, and M. Weidemüller, *Phys. Rev. Lett.* **93**, 163001 (2004).
- [7] R. Heidemann, U. Raitzsch, V. Bendkowsky, B. Butscher, R. Löw, L. Santos, and T. Pfau, *Phys. Rev. Lett.* **99**, 163601 (2007).
- [8] T. D. Ladd, F. Jelezko, R. Laflamme, Y. Nakamura, C. Monroe, and J. L. O’Brien, *Nat. Phys.* **464**, 45 (2010).
- [9] M. Saffman, T. G. Walker, and K. Mølmer, *Rev. Mod. Phys.* **82**, 2313 (2010).
- [10] P. Bellomo and C. R. S. Jr., *Phys. Rev. A* **59**, 2139 (1999).
- [11] J. M. Raimond, M. Brune, and S. Haroche, *Rev. Mod. Phys.* **73**, 566 (2001).
- [12] J. C. Day, T. Ehrenreich, S. B. Hansen, E. Horsdal-Pedersen, K. S. Mogensen, and K. Taulbjerg, *Phys. Rev. Lett.* **72**, 1612 (1994).
- [13] R. Lutwak, J. Holley, P. P. Chang, S. Paine, D. Kleppner, and T. Ducas, *Phys. Rev. A* **56**, 1443 (1997).
- [14] M. Forre, H. M. Nilsen, and J. P. Hansen, *Phys. Rev. A* **65**, 053409 (2002).
- [15] A. Kazansky and V. Ostrovsky, *J. Phys. B* **29**, L855 (1996).
- [16] E. Majorana, *Nuovo Cimento* **9**, 43 (1932).
- [17] Y. V. Vanne, A. Saenz, A. Dalgarno, R. C. Forrey, P. Froelich, and S. Jonsell, *Phys. Rev. A* **73**, 062706 (2006).
- [18] Full movies of the time development of the electron density in the xz plane can be downloaded from [<http://web.ift.uib.no/janp/Rydbergmovies>].
- [19] S. D. Hogan, C. Seiler, and F. Merkt, *Phys. Rev. Lett.* **103**, 123001 (2009).
- [20] E. Waltersson, E. Lindroth, I. Piskog, and J. P. Hansen, *Phys. Rev. B* **79**, 115318 (2009).